Chapter 5

Network-Constrained Peer-to-Peer Energy Transactions: A Cooperative Game Analysis Framework

5.1 Introduction

The previous chapter addresses non-cooperative game-based P2P trading without considering the distribution network constraints. This chapter proposes a cloud computing-based novel P2P energy trading framework consisting of virtual communities (VCs) created by a hypothetical aggregation of buildings on a particular bus. The proposed framework can potentially settle transactions regarding network constraints by using dynamic network usage charges and electricity tariffs. A cooperative game is designed for intra- and inter-bus energy trading that considers the unequal contribution of each participant in the coalition for an incentive distribution. In this work, each player's objective function is decoupled to achieve equilibrium in a decentralised manner. Each VC is equipped with a shareable battery energy storage. For a more realistic scenario, a stochastic model is used to deal with the uncertainties related to RESs. The proposed framework features a cloud-based computing setup to avoid the security and privacy issues that would normally be present in any data-intensive task. In addition to the framework discussed in the previous chapters, the following additional contributions are made in this chapter.

The above-mentioned contributions of this chapter can be summarized as follows.

- The proposed decentralized P2P framework fine-tunes the transactions in regard to the

technical constraints using the dynamic network usage charges and electricity tariffs.

- To enable the framework discussed in this chapter, an entity called DSO has been introduced.
- For incentive distribution in this framework, a cooperative game is proposed, and the resulting game is solved using a Nash bargaining solution in a decentralized manner.
- Furthermore, this study considers the uncertainties in renewable energy generation, thus reinforcing its commitment to practical applicability.

5.2 Problem Formulation

This section discusses the elements involved in the problem formulation, such as system architecture, objectives at building and at the level of virtual communities, and DSO.

5.2.1 System Architecture

In this work, all the neighbouring buildings and BESS on a single bus (Figure 5.1) are grouped to form virtual communities (VCs). Here, VC is nothing but a hypothetical aggregation of shareable BESS and buildings connected through a computing cloud. Smart metering and a robust communication system are assumed to be present for monitoring and operation of demand-responsive loads and RESs for buildings. For the implementation of limited information sharing, a separate and secure cloud platform is assumed to be present for each internal energy trading (i.e. building-to-building (B2B), building-to-community (B2C), and community-to-community (C2C)). In each VC, cloud computing is used to handle the coupling decisions of buildings and BESS that are required for B2B and B2C trading, charging/discharging of BESS, and trading with other VCs and the utility.

The VC considered here is a non-profit based for its buildings and profit based with respect to other VCs for C2C trading. This concept utilizes the advantage of P2P sharing of all buildings with less communication and computational burden [65] and without affecting the overall benefits of the buildings. In the process of this internal P2P trading, the network parameters may violate the network constraints. An independent operator, DSO, ensures that all the network parameters are maintained within limits with the help of a dynamic Network Utilization Cost (NUC).

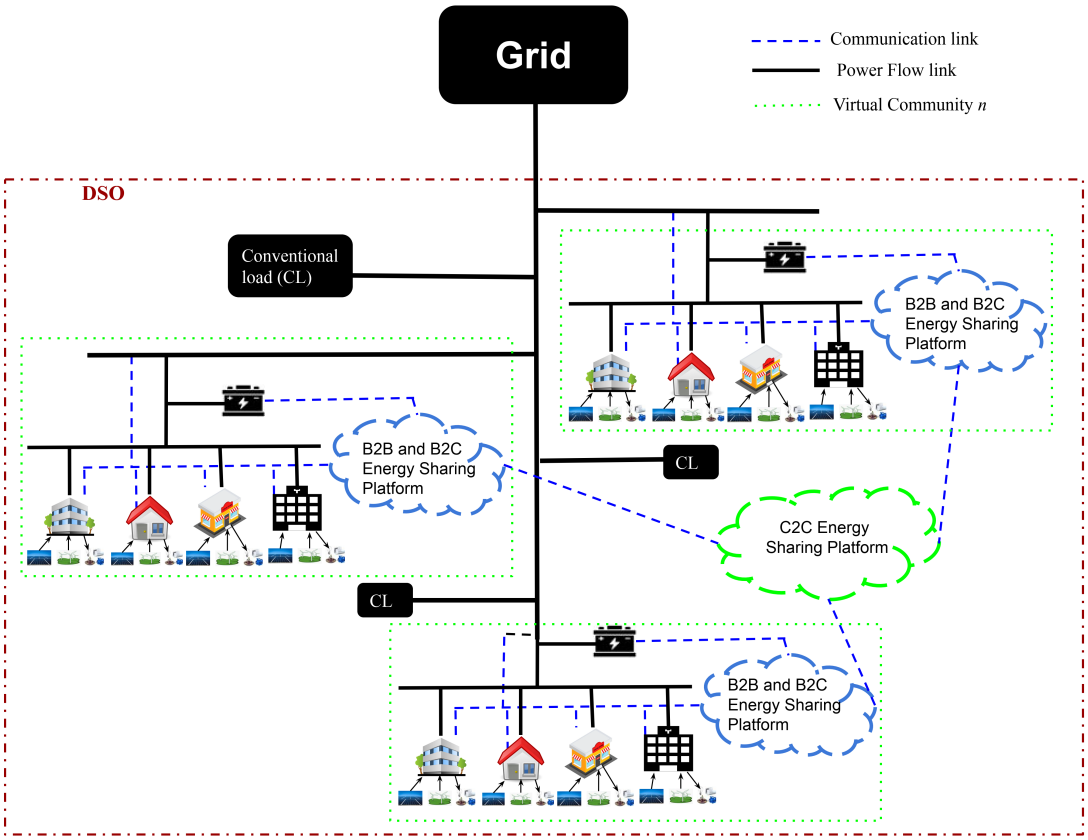

Figure 5.1: PEER-TO-PEER ENERGY SHARING FRAMEWORK

Table 5.1: DETAIL OF DATA EXCHANGE DURING INTERNAL TRANSACTIONS

Sr. no.	Type of Internal Transactions	Data Given to theCloud	Data Received from the Cloud
1	B2B	B2B Power and Incentives	Corresponding Auxiliary Variables
2	B2C	B2C Power and Incentives	Corresponding Auxiliary Variables
3	C2C	C2C Power and Incentives	Corresponding Auxiliary Variables

In the face of a progressively expanding environment, the burden carried by the communication infrastructure is undeniably enhanced, resulting in a simultaneous increase in computational complexities [65]. Also, for communication with DSO, either each building does it directly or an aggregator at each bus is present for this communication in the existing literature. The diverse challenges explored in this work are methodically resolved by harnessing the capabilities of virtual communities (VCs), which are the hypothetical gathering of all the buildings of each bus. The conventional practice of distributing Battery Energy Storage Systems (BESS) within individual building units is replaced by a more coordinated approach, whereby a designated group of buildings shares BESS. The concept of virtual communities facilitates the orchestration of this collaborative configuration.

From Table 5.1, it can be observed that it is impossible to infer the exact load demand or RES generation of the buildings. The buildings optimise their problem using the auxiliary variables received from the cloud and give back the optimised output to the cloud. Thus, the buildings' data is preserved, and privacy issues are avoided.

5.2.2 Problem Formulation: Building Level

Each building incorporates load shifting as demand-side management to reduce its cost. However, the discomfort experienced by the consumer due to this load shifting is considered as cost in the objective function of buildings. Apart from this, all the buildings are involved in B2B and B2C energy trading. So, the cost function of i^{th} building in n^{th} VC, $C^{b}_{n,i}$ can be defined as,

$$C^{b}_{n,i} = \sum_{t=1}^{T} C^{ls}_{n,i,t} + C^{b2b}_{n,i} + C^{b2c}_{n,i}. \tag{5.1}$$

5.2.2.1 Load Shifting

The consumer discomfort cost, $C^{ls}_{n,i,t}$, due to load-shifting can be given by

$$C^{ls}_{n,i,t} = \Lambda^{dis}_t (P^{ls}_{n,i,t} - L_{n,i,t})^2. \tag{5.2}$$

Here, Λ^{dis}_t is the weighted coefficient for discomfort due to shifting from actual load $L_{n,i,t}$ to load pattern $P^{ls}_{n,i,t}$. The load shifting is subjected to the following constraints.

$$L^{min}_{n,i,t} \leq P^{ls}_{n,i,t} \leq L^{max}_{n,i,t}, \qquad and \tag{5.3}$$

$$\sum_{t=1}^{T} P^{ls}_{n,i,t} \geq \epsilon^{LS} \sum_{t=1}^{T} L_{n,i,t}. \tag{5.4}$$

The equation (5.3) limits the demand after load shifting. At a time instant, the load cannot be increased or decreased beyond a particular limit. The maximum allowable load curtailment is constrained by (5.4). ϵ^{LS} represents the fraction of load supplied. ϵ^{LS} equals 1 represents the no load-curtailment.

5.2.2.2 B2B and B2C Energy Exchange

Buildings share energy with other buildings ($P^{b2b}_{n,i,j,t}$) and with the VC ($P^{b2c}_{n,i,t}$). Both ($P^{b2b}_{n,i,j,t}$) and ($P^{b2c}_{n,i,t}$) have positive values in the case of imports and negative for exports. To motivate the prosumers for these internal energy trading, incentives $\pi^{b2b}_{n,i,j}$ and $\pi^{b2c}_{n,i}$ are provided for B2B and B2C energy trading, such that,

$$C^{b0}_{n,i} - C^{b}_{n,i} \geq 0. \tag{5.5}$$

Here, $C^{b0}_{n,i}$ is the cost for the i^{th} buildings of n^{th} VC in the absence of B2B and B2C energy trading. The incentives $\pi^{b2b}_{n,i,j}$ and $\pi^{b2c}_{n,i}$ are positive in case the building is paying, and else these are negative. The cost of B2B trading, $C^{b2b}_{n,i}$ and B2C trading, $C^{b2c}_{n,i}$ can be defined as,

$$C^{b2b}_{n,i} = \sum_{j=1,\ j\neq i}^{N^b_n} \pi^{b2b}_{n,i,j}, \text{ and } C^{b2c}_{n,i} = \pi^{b2c}_{n,i}.$$

Here N^b_n is the number of buildings in n^{th} VC. The power and incentive balance for a B2B transaction between i^{th} and j^{th} building in n^{th} VC can be written as follows.

$$P^{b2b}_{n,i,j,t} + P^{b2b}_{n,j,i,t} = 0, \qquad and \tag{5.6}$$

$$\pi^{b2b}_{n,i,j} + \pi^{b2b}_{n,j,i} = 0. \tag{5.7}$$

The constraints (5.6) and (5.7) are the coupling constraints between i^{th} and j^{th} building in n^{th} VC because they contain the decision variables of both the buildings. Considering RES generation,$R_{n,i,t}$, the load balancing equation for a building can be defined as,

$$-\sum_{\substack{j=1 \\ j\neq i}}^{N_n^b} P_{n,i,j,t}^{b2b} - P_{n,i,t}^{b2c} = R_{n,i,t} - P_{n,i,t}^{ls}. \tag{5.8}$$

5.2.3 Problem Formulation: Virtual Community Level

After considering the power exchange request of all the buildings in its premises, the decision to trade energy with the utility and other VCs and the decision of charging/discharging of BESS is taken in the computing cloud of the VC. The cost function of a VC includes the cost of energy exchange with the utility $C_{n,t}^{U}$, the cost of energy exchange with other VCs C_{n}^{c2c}, and the cost of BESS utilization $C_{n,t}^{BESS}$, which be represented as,

$$C_n^c = \sum_{t=1}^{T}(C_{n,t}^{U} + C_{n,t}^{BESS}) + C_n^{c2c}. \tag{5.9}$$

In this work, the VC acts as a non-profit based entity with respect to its buildings. Therefore, the B2C exchange cost is not considered in the objective function, C_n^c i.e. cost of VC and this cost of the VC is shared by the buildings of that VC as follows.

$$C_n^c = \sum_{i=1}^{N_n^b} \pi_{n,i}^{b2c}. \tag{5.10}$$

5.2.3.1 Exchange with the Utility

The cost of energy exchange with the utility can be defined as,

$$C_{n,t}^{U} = (\Lambda_{n,t}^{im} + \epsilon^{CE})P_{n,t}^{b} - \Lambda_{n,t}^{ex}P_{n,t}^{s}. \tag{5.11}$$

Here, $P_{n,t}^{b}$ and $P_{n,t}^{s}$ are the power import and export from the utility, and ϵ^{CE} is the charges due to carbon emission. The power import price for a VC, $\Lambda_{n,t}^{im}$, is based on the LMP of the bus k containing that VC, such that $\Lambda_{n,t}^{im} = a\lambda_{t,k}^{LMP}$. The term a is a scale factor decided by the utility. The power export price, $\Lambda_{n,t}^{ex}$ is considered as $\Lambda_{t}^{ex} = \Lambda_{t}^{im}/\epsilon^{R}$, where ϵ^{R} is the ratio of price of import and export.

5.2.3.2 Battery Energy Storage System (BESS)

The repetitive charging/discharging will degrade the quality of BESS. The BESS utilization cost in terms of BESS utilization coefficient, Λ^{UTI}, and charging/discharging powers, $P^{ch}_{n,t}$ and $P^{dis}_{n,t}$, can be written as,

$$C^{BESS}_{n,t} = \Lambda^{UTI}(P^{ch}_{n,t} + P^{dis}_{n,t}). \tag{5.12}$$

The charging power, $P^{ch}_{n,t}$, and discharging power, $P^{dis}_{n,t}$, of the BESS are constrained as follows.

$$P^{ch_{min}}_{n} \leq P^{ch}_{n,t} \leq P^{ch_{max}}_{n}, \qquad and \tag{5.13}$$

$$P^{dis_{min}}_{n} \leq P^{dis}_{n,t} \leq P^{dis_{max}}_{n}. \tag{5.14}$$

State-of-charge (SOC) at time t, $SOC_{n,t}$, of BESS depends on the SOC at time t-1, $SOC_{n,t-1}$, and charging/discharging powers status, which can be written as

$$SOC_{n,t} = (1 - \eta^{loss}_{n})SOC_{n,t-1} + \eta^{ch}_{n}P^{ch}_{n,t} - \frac{1}{\eta^{dis}_{n}}P^{dis}_{n,t}, \qquad and \tag{5.15}$$

$$SOC^{min}_{n} \leq SOC_{n,t} \leq SOC^{max}_{n}, \tag{5.16}$$

where, η^{ch}_{n}/η^{dis}_{n} and η^{loss}_{n} are the charging/discharging efficiency and parameter associated with self-discharging of the battery.

5.2.3.3 C2C trading

Inter-community power exchange, $P^{c2c}_{n,m,t}$, provides an opportunity to reduce the electricity cost and increase the use of RES. In the case of power transfer from m^{th} VC to n^{th} VC, ($P^{c2c}_{n,m,t}$) is positive else negative. Corresponding to this power exchange, the VC will get/give incentives $\pi^{c2c}_{n,m}$ from/to other VCs. If n^{th} VC has to pay $\pi^{c2c}_{n,m}$ to m^{th} VC , then $\pi^{c2c}_{n,m}$ is positive, else it will be negative. The VC has to pay a Network Utilization Cost (NUC) for C2C power exchange. The NUC can be written as,

$$C^{NUC}_{n,m,t} = \Lambda^{NUC}_{n,m,t}P^{c2c^{aux}}_{n,m,t}. \tag{5.17}$$

where,

$$\Lambda^{NUC}_{n,m,t} = \begin{cases} \frac{1}{2}max(\lambda^{LMP}_{t,n} - \lambda^{LMP}_{t,m}) & \text{if } P^{c2c}_{n,m,t} \geq 0 \text{ and } (\lambda^{LMP}_{t,n} - \lambda^{LMP}_{t,m}) \geq 0\,, \\ 0 & \text{if } P^{c2c}_{n,m,t} \geq 0 \text{ and } (\lambda^{LMP}_{t,n} - \lambda^{LMP}_{t,m}) < 0\,, \\ \frac{1}{2}max(\lambda^{LMP}_{t,m} - \lambda^{LMP}_{t,n}) & \text{if } P^{c2c}_{n,m,t} < 0 \text{ and } (\lambda^{LMP}_{t,m} - \lambda^{LMP}_{t,n}) \geq 0\,, \\ 0 & \text{if } P^{c2c}_{n,m,t} < 0 \text{ and } (\lambda^{LMP}_{t,m} - \lambda^{LMP}_{t,n}) < 0\,. \end{cases}$$

According to the above equation, the Network Utilization Charge (NUC) is applied when power is exported from a higher LMP bus to a lower LMP bus. The LMPs are determined using Optimal Power Flow (OPF), which considers voltage levels, line limits, and other relevant factors. If a peer-to-peer (P2P) energy exchange violates any system constraints, this is reflected in the LMP, leading to an increase in the NUC. The higher NUC then discourages excessive power exchange, prompting communities to adjust their exchanged power values. These updated values are subsequently used in the next OPF calculation. This iterative process continues until the difference between successive LMP values falls within an acceptable tolerance. In this way, the NUC helps manage line loading and voltage limits effectively.

Also, the auxiliary variable, $P_{n,m,t}^{c2c^{aux}}$, is used to for extracting the magnitude only i.e. when $P_{n,m,t}^{c2c^{aux}} \geq -P_{n,m,t}^{c2c}$, $P_{n,m,t}^{c2c^{aux}} \geq P_{n,m,t}^{c2c}$ and $P_{n,m,t}^{c2c^{aux}} \geq 0$. For power import, the price for network utilization, $\Lambda_{n,m,t}^{NUC}$, in C2C energy trading is half of the difference in the LMPs of the bus containing n^{th} and m^{th} VC. But for power export, $\Lambda_{n,m,t}^{NUC}$ is half of the difference in the LMPs of the bus containing m^{th} and n^{th} VC. In case this difference is negative, then $\Lambda_{n,m,t}^{NUC} = 0$. The LMP of the bus k is denoted by $\lambda_{t,k}^{LMP}$. The constraints related to the C2C energy exchange are as follows.

$$P_{n,m,t}^{c2c} + P_{m,n,t}^{c2c} = 0, \tag{5.18}$$

$$\pi_{n,m}^{c2c} + \pi_{m,n}^{c2c} = 0, \qquad and \tag{5.19}$$

$$C_n^{c0} - C_n^{c} \geq 0. \tag{5.20}$$

Here, C_n^{c0} is the cost of the n^{th} VC in the absence of C2C energy trading. The incentives are decided based on (5.20). Thus, the total C2C cost is given by,

$$C_n^{c2c} = \sum_{\substack{m=1 \\ m \neq n}}^{N^C} (\sum_{t=1}^{T} C_{n,m,t}^{NUC} + \pi_{n,m}). \tag{5.21}$$

Here, N^C is the number of VCs. The load balancing equation concerning the VC can be given as,

$$P_{n,t}^{b} - P_{n,t}^{s} + P_{n,t}^{dis} - P_{n,t}^{ch} + \sum_{\substack{m=1 \\ m \neq n}}^{N^C} P_{n,m,t}^{c2c} = \sum_{i=1}^{N_n^b} P_{n,i,t}^{b2c}. \tag{5.22}$$

This framework doesn't need any separate constraints to prevent simultaneous charging and discharging or buying and selling to the grid, as explained in Appendix III.

5.2.4 Problem Formulation: DSO Level

The DSO is responsible for maintaining the network constraints. It does so by determining the LMPs based on optimal power flow. The objective function of DSO can be defined as,

$$C^{DSO} = \sum_{t=1}^{T} [\Lambda_t^{G,P} P_{1,t}^G + \Lambda_t^{G,Q} \left|Q_{1,t}^G\right| + \sum_{d=1}^{N^{DG}} (\Lambda_{d,t}^{DG,P} P_{d,t}^{DG} + \Lambda_{d,t}^{DG,Q} \left|Q_{d,t}^{DG}\right|)]. \tag{5.23}$$

Here, $P_{1,t}^G$ and $Q_{1,t}^G$ are active and reactive power exchange with grid (bus1) and $\Lambda_t^{G,P}$ and $\Lambda_t^{G,Q}$ are corresponding prices. $P_{d,t}^{DG}$ and $Q_{d,t}^{DG}$ are the active and reactive power supplied by DG, and their respective prices are $\Lambda_{d,t}^{DG,P}$ and $\Lambda_{d,t}^{DG,Q}$. The $\left|Q_{1,t}^G\right|$ can make the problem non-convex. So, instead of $\left|Q_{1,t}^G\right|$, in this framework $Q_{1,t}^{G^{aux}}$ is used in this framework such that $Q_{1,t}^{G^{aux}} \geq -Q_{1,t}^G$, $Q_{1,t}^{G^{aux}} \geq Q_{1,t}^G$ and $Q_{1,t}^{G^{aux}} \geq 0$.

The network constraints for the distribution system can be defined as follows.

$$\sum_{k=1}^{N^B} P_{k,t}^G - \sum_{k=1}^{N^B} P_{k,t}^D = 0 \quad : \lambda_t^1 \tag{5.24}$$

$$\sum_{k=1}^{N^B} Q_{k,t}^G - \sum_{k=1}^{N^B} Q_{k,t}^D = -\sum_{k'=1}^{N^B} b_{k'k'} \quad : \lambda_t^2 \tag{5.25}$$

The constraints (5.24) and (5.25) denote the active and reactive power balance for each time interval and here N^B is the number of buses. The total active power generation and demand at bus k can be defined as,

$$P_{k,t}^G = x_k^{PCC} P_t^G + \sum_{d=1}^{N^{DG}} x_{d,k}^{DG} P_{d,t}^{DG}, \quad and \tag{5.26}$$

$$P_{k,t}^D = P_{k,t}^{FD} + \sum_{n=1}^{N^C} x_{n,k}^C P_t^{net,n}. \tag{5.27}$$

Here, x_k^{PCC}, $x_{d,k}^{DG}$, and $x_{n,k}^C \in \{0, 1\}$, are the binary parameters to indicate the connection of Point of Common Coupling (PCC), DG, and VC respectively at k^{th} bus. The term $P_t^{net,n}$ represents the net injection of n^{th} VC, which includes power exchange with utility and power exchange with other VCs. Similarly, the total reactive power generation and demand can be defined for all buses.

The equation (5.28) constrains the line flow within limits.

$$-P_l^{max} \leq \sum_{k=1}^{N^B} f_{l-k}^{P-P}(P_{k,t}^G - P_{k,t}^D) + \sum_{k=1}^{N^B} f_{l-k}^{P-Q}(Q_{k,t}^G - Q_{k,t}^D) \leq P_l^{max} \quad : \mu_{l,t}^1, \mu_{l,t}^2 \quad \forall l \tag{5.28}$$

$$V^{min} \leq \sum_{k=1}^{N^B} X_{N^B+k',k}(P^G_{k,t} - P^D_{k,t}) + \sum_{k=1}^{N^B} X_{N^B+k',N^B+k}$$
$$(Q^G_{k,t} - Q^D_{k,t}) \leq V^{max} : \mu^3_{k',t}, \mu^4_{k',t} \ \forall k' \quad (5.29)$$

Parameters f^{P-P}_{l-k} and f^{P-Q}_{l-k} are the Generation Shift Distribution (GSD) factors for l^{th} line. The detailed derivations of GSD factors are given in Appendix I, which is taken from [81]. The voltage magnitude at each bus is constrained by (5.29). The term $X_{*,*}$ depends on the network topology as described in Appendix I.

Similarly, the other network constraints are specified as follows.

$$P^{G,min} \leq P^G_t \leq P^{G,max} : \mu^5_t, \mu^6_t \quad (5.30)$$

$$Q^{G,min} \leq Q^G_t \leq Q^{G,max} : \mu^7_t, \mu^8_t \quad (5.31)$$

$$P^{DG,min}_d \leq P^{DG}_{d,t} \leq P^{DG,max}_d : \mu^9_{t,d}, \mu^{10}_{t,d} \quad \forall d \quad (5.32)$$

$$Q^{DG,min}_d \leq Q^{DG}_{d,t} \leq Q^{DG,max}_d : \mu^{11}_{t,d}, \mu^{12}_{t,d} \quad \forall d \quad (5.33)$$

The constraints (5.30) and (5.31) are used to limit active and reactive power demand at PCC, while constraints (5.32) and (5.33) are used to limits active and reactive generation of DGs. The Lagrangian function for the DSO level can be written as given in the equation [1]. The active power LMP at k^{th} can be determined using a partial derivation of the Lagrangian function

[1]

$$\begin{aligned}
L = \sum_{t=1}^{T} \Big[& C^{DSO} - \lambda^1_t(\sum_{k=1}^{N^B} P^G_{k,t} - \sum_{k=1}^{N^B} P^D_{k,t}) - \lambda^2_t(\sum_{k=1}^{N^B} Q^G_{k,t} - \sum_{k=1}^{N^B} Q^D_{k,t} + \sum_{k'=1}^{N^B} b_{k'k'}) \\
& - \sum_l \mu^1_{l,t}(-P^{max}_l - \sum_{k=1}^{N^B} f^{P-P}_{l-k}(P^G_{k,t} - P^D_{k,t}) - \sum_{k=1}^{N^B} f^{P-Q}_{l-k}(Q^G_{k,t} - Q^D_{k,t})) \\
& - \sum_l \mu^2_{l,t}(-P^{max}_l + \sum_{k=1}^{N^B} f^{P-P}_{l-k}(P^G_{k,t} - P^D_{k,t}) + \sum_{k=1}^{N^B} f^{P-Q}_{l-k}(Q^G_{k,t} - Q^D_{k,t})) \\
& - \sum_{k'} \mu^3_{k',t}(V^{min} - \sum_{k=1}^{N^B} X_{N^B+k',k}(P^G_{k,t} - P^D_{k,t}) - \sum_{k=1}^{N^B} X_{N^B+k',N^B+k}(Q^G_{k,t} - Q^D_{k,t})) \\
& - \sum_{k'} \mu^4_{k',t}(-V^{max} + \sum_{k=1}^{N^B} X_{N^B+k',k}(P^G_{k,t} - P^D_{k,t}) + \sum_{k=1}^{N^B} X_{N^B+k',N^B+k}(Q^G_{k,t} - Q^D_{k,t})) \\
& - \mu^5_t(P^G_{min} - P^G_t) - \mu^6_t(-P^G_{max} + P^G_t) - \mu^7_t(Q^G_{min} - Q^G_t) - \mu^8_t(-Q^G_{max} + Q^G_t) \\
& - \sum_d \mu^9_{t,d}(P^d_{min} - P^d_t) - \mu^{10}_{t,d}(-P^d_{max} + P^d_t) - \sum_d \mu^{11}_{t,d}(Q^d_{min} - Q^d_t) - \mu^{12}_{t,d}(-Q^d_{max} + Q^d_t) \Big]
\end{aligned}$$

with respect to the power demand of k^{th} bus. The active power LMP for k^{th} bus can be written as

$$\lambda_{t,k}^{LMP} = \lambda_t^1 + \sum_l (-\mu_{l,t}^1 + \mu_{l,t}^2) f_{l-k}^{P-P} + \sum_{k'} (-\mu_{k',t}^3 + \mu_{k',t}^4) X_{N^B+k',k}. \tag{5.34}$$

The reactive power LMP is not considered in this work, as the reactive power demands of VCs are considered zero.

5.3 Methodology

The uncertainties due to RESs (solar and wind generation) are dealt with Hong's 2m Point Estimate Method (PEM) [77] as described in Section 2.9. This method considers the uncertainties of RESs and gives the expected value of energy scheduling. In subsequent sections, only the cost function is denoted by $\mathbb{E}(.)$ instead of all variables for simplicity. A cooperative game is formulated in section 5.3.1, which is then solved using the Alternating Direction Method of Multipliers (ADMM) for decentralised optimisation.

5.3.1 Nash Bargaining game formulation

A cooperative game for the problem described in section 5.2 can be formed as given in Table 5.2. The game is played in two levels due to the presence of B2C coupled variables.

Table 5.2: DESCRIPTION OF THE COOPERATIVE GAME

Levels	Players	Strategies	Objectives
1	Buildings	$X_{n,i,t}^b := (P_{n,i,t}^{ls}, P_{n,i,j,t}^{b2b}, P_{n,i,t}^{b2c}, \pi_{n,i,j}^{b2b}, \pi_{n,i}^{b2c})$	$C_{n,i}^b$
2	VCs	$X_{n,t}^c := (P_{n,t}^b, P_{n,t}^s, P_{n,t}^{ch}, P_{n,t}^{dis}, P_{n,m,t}^{c2c}, \pi_{n,m}^{c2c})$	C_n^c

A Nash Bargaining Problem (NBP) is formulated to find the Nash equilibrium of this cooperative game such that the expected cost saving is distributed among the participants. Thus, the required NBP is

$$\mathscr{F}_1 : \ max[\prod_{n=1}^{N^C} \{\prod_{i=1}^{N_n^b} (\mathbb{E}(C_{n,i}^{b0}) - \mathbb{E}(C_{n,i}^b))(\mathbb{E}(C_n^{c0}) - \mathbb{E}(C_n^c))\}]. \tag{5.35}$$

The aforementioned maximization problem can be transformed into a minimization problem as,

$$\mathscr{F}_2 : \ min[-\sum_{n=1}^{N^C} \{\sum_{i=1}^{N_n^b} log(1 + \mathbb{E}(C_{n,i}^{b0}) - \mathbb{E}(C_{n,i}^b)) + log(1 + \mathbb{E}(C_n^{c0}) - \mathbb{E}(C_n^c))\}]. \tag{5.36}$$

The above problem can be solved in a decentralised manner using ADMM [76] by decoupling the "coupling constraints" given by (5.6),(5.7),(5.18),(5.19),(5.22), and (5.10). For decoupling, the auxiliary variables ($\sigma^{P_{b2b}}_{n,i,j,t}$, $\sigma^{\pi_{b2b}}_{n,i,j}$, $\sigma^{P_{c2c}}_{n,m,t}$, $\sigma^{\pi_{c2c}}_{n,m}$, $\sigma^{P_{b2c}}_{n,i,t}$, and $\sigma^{\pi_{b2c}}_{n,i}$) are employed for $P^{b2b}_{n,i,j,t}$, $\pi^{b2b}_{n,i,j}$, $P^{c2c}_{n,m,t}$, $\pi^{c2c}_{n,m}$, $P^{b2c}_{n,i,t}$, and $\pi^{b2c}_{n,i}$, respectively.

Now the coupling constraints can be reformulated as follows,

$$\sigma^{P_{b2b}}_{n,i,j,t} + \sigma^{P_{b2b}}_{n,j,i,t} = 0, \tag{5.37}$$

$$\sigma^{\pi_{b2b}}_{n,i,j} + \sigma^{\pi_{b2b}}_{n,j,i} = 0, \tag{5.38}$$

$$\sigma^{P_{c2c}}_{n,m,t} + \sigma^{P_{c2c}}_{m,n,t} = 0, \tag{5.39}$$

$$\sigma^{\pi_{c2c}}_{n,m} + \sigma^{\pi_{c2c}}_{m,n} = 0, \tag{5.40}$$

$$P^{b}_{n,t} - P^{s}_{n,t} + P^{dis}_{n,t} - P^{ch}_{n,t} + \sum_{\substack{m=1 \\ m\neq n}}^{N^C} P^{c2c}_{n,m,t} = \sum_{i=1}^{N^b_n} \sigma^{P_{b2c}}_{n,i,t}, \quad \textit{and} \tag{5.41}$$

$$C^{c}_{n} = \sum_{i=1}^{N^b_n} \sigma^{\pi_{b2c}}_{n,i}. \tag{5.42}$$

The equation (5.36) can be re-formulated depending upon the reformulation of coupling constraints as follows.

$$\begin{aligned}
\mathscr{F}_3 :\ min\Bigg(& \Big[- \sum_{n=1}^{N^C} \Big\{ \sum_{i=1}^{N^b_n} log(1 + \mathbb{E}(C^{b0}_{n,i}) - \mathbb{E}(C^{b}_{n,i})) + log(1 + \mathbb{E}(C^{c0}_{n}) - \mathbb{E}(C^{c}_{n})) \Big\} \Big] \\
& + \sum_{n=1}^{N^C} \sum_{i=1}^{N^b_n} \sum_{\substack{j=1 \\ j\neq i}}^{N^b_n} \Big[\sum_{t=1}^{T} \frac{\delta_1}{2} (P^{b2b}_{n,i,j,t} - \sigma^{P_{b2b}}_{n,i,j,t} + \frac{\omega^{P_{b2b}}_{n,i,j,t}}{\delta_1})^2 + \frac{\delta_2}{2} (\pi^{b2b}_{n,i,j} - \sigma^{\pi_{b2b}}_{n,i,j} + \frac{\omega^{\pi_{b2b}}_{n,i,j}}{\delta_2})^2 \Big] \\
& + \sum_{n=1}^{N^C} \sum_{i=1}^{N^b_n} \Big[\sum_{t=1}^{T} \frac{\delta_3}{2} (P^{b2c}_{n,i,t} - \sigma^{P_{b2c}}_{n,i,t} + \frac{\omega^{P_{b2c}}_{n,i,t}}{\delta_3})^2 + \frac{\delta_4}{2} (\pi^{b2c}_{n,i} - \sigma^{\pi_{b2c}}_{n,i} + \frac{\omega^{\pi_{b2c}}_{n,i}}{\delta_4})^2 \Big] \\
& + \sum_{n=1}^{N^C} \sum_{\substack{m=1 \\ m\neq n}}^{N^C} \Big[\sum_{t=1}^{T} \frac{\delta_5}{2} (P^{c2c}_{n,m,t} - \sigma^{P_{c2c}}_{n,m,t} + \frac{\omega^{P_{c2c}}_{n,m,t}}{\delta_5})^2 + \frac{\delta_6}{2} (\pi^{c2c}_{n,m} - \sigma^{\pi_{c2c}}_{n,m} + \frac{\omega^{\pi_{c2c}}_{n,m}}{\delta_6})^2 \Big] \Bigg).
\end{aligned} \tag{5.43}$$

The variables for the above problem are X^b and X^c (as described in the strategies of the cooperative game so formulated). Apart from them, the other variables are σs, ωs, and δs. This problem is constrained by γ_b, γ_c, γ_1, and γ_2. Here, γ_b :=[(5.3) to (5.5), (5.8)], γ_c :=[$P^s \geq 0$, $P^b \geq 0$, (5.13) to (5.16), (5.20), (5.41),(5.42)], γ_1 :=[(5.37), (5.38)], and γ_2 :=[(5.39), (5.40)].

In the n^{th} VC for i^{th} building, (5.43) can be re-written as,

$$\mathscr{F}_4: \ min\Bigg(-log\big(1+\mathbb{E}(C^{b0}_{n,i})-\mathbb{E}(C^{b}_{n,i})\big) + \sum_{\substack{j=1\\ j\neq i}}^{N^b_n}\Big[\sum_{t=1}^{T}\frac{\delta_1}{2}(P^{b2b}_{n,i,j,t}-\sigma^{P_{b2b}}_{n,i,j,t}+\frac{\omega^{P_{b2b}}_{n,i,j,t}}{\delta_1})^2+\frac{\delta_2}{2}(\pi^{b2b}_{n,i,j}-\sigma^{\pi_{b2b}}_{n,i,j}+\frac{\omega^{\pi_{b2b}}_{n,i,j}}{\delta_2})^2\Big] + \sum_{t=1}^{T}\frac{\delta_3}{2}(P^{b2c}_{n,i,t}-\sigma^{P_{b2c}}_{n,i,t}+\frac{\omega^{P_{b2c}}_{n,i,t}}{\delta_3})^2+\frac{\delta_4}{2}(\pi^{b2c}_{n,i}-\sigma^{\pi_{b2c}}_{n,i}+\frac{\omega^{\pi_{b2c}}_{n,i}}{\delta_4})^2\Bigg). \quad (5.44)$$

For B2B auxiliary variables for n^{th} VC, updated equation (5.43) can be re-written as,

$$\mathscr{F}_5: \ min\Bigg(\sum_{i=1}^{N^b_n}\sum_{\substack{j=1\\ j\neq i}}^{N^b_n}\Big[\sum_{t=1}^{T}\frac{\delta_1}{2}(P^{b2b}_{n,i,j,t}-\sigma^{P_{b2b}}_{n,i,j,t}+\frac{\omega^{P_{b2b}}_{n,i,j,t}}{\delta_1})^2+\frac{\delta_2}{2}(\pi^{b2b}_{n,i,j}-\sigma^{\pi_{b2b}}_{n,i,j}+\frac{\omega^{\pi_{b2b}}_{n,i,j}}{\delta_2})^2\Big]\Bigg). \quad (5.45)$$

At the level of n^{th} VC, (5.43) can be re-written as,

$$\mathscr{F}_6: \ min\Bigg(-log(1+\mathbb{E}(C^{c0}_{n})-\mathbb{E}(C^{c}_{n})) + \sum_{i=1}^{N^b_n}\Big[\sum_{t=1}^{T}\frac{\delta_3}{2}(P^{b2c}_{n,i,t}-\sigma^{P_{b2c}}_{n,i,t}+\frac{\omega^{P_{b2c}}_{n,i,t}}{\delta_3})^2+\frac{\delta_4}{2}(\pi^{b2c}_{n,i}-\sigma^{\pi_{b2c}}_{n,i}+\frac{\omega^{\pi_{b2c}}_{n,i}}{\delta_4})^2\Big] + \sum_{\substack{m=1\\ m\neq n}}^{N^C}\Big[\sum_{t=1}^{T}\frac{\delta_5}{2}(P^{c2c}_{n,m,t}-\sigma^{P_{c2c}}_{n,m,t}+\frac{\omega^{P_{c2c}}_{n,m,t}}{\delta_5})^2+\frac{\delta_6}{2}(\pi^{c2c}_{n,m}-\sigma^{\pi_{c2c}}_{n,m}+\frac{\omega^{\pi_{c2c}}_{n,m}}{\delta_6})^2\Big]\Bigg). \quad (5.46)$$

For C2C auxiliary variables update, (5.43) can be re-written as,

$$\mathscr{F}_7: \ min\Bigg(\sum_{n=1}^{N^C}\sum_{\substack{m=1\\ m\neq n}}^{N^C}\Big[\sum_{t=1}^{T}\frac{\delta_5}{2}(P^{c2c}_{n,m,t}-\sigma^{P_{c2c}}_{n,m,t}+\frac{\omega^{P_{c2c}}_{n,m,t}}{\delta_5})^2+\frac{\delta_6}{2}(\pi^{c2c}_{n,m}-\sigma^{\pi_{c2c}}_{n,m}+\frac{\omega^{\pi_{c2c}}_{n,m}}{\delta_6})^2\Big]\Bigg). \quad (5.47)$$

The flowchart of energy scheduling is presented in Figure 5.2. The λ^P and λ^D refer to primal and dual residuals, and (κ, ν) are given constants. After initialization, each player at the building level will simultaneously optimize its strategies, and then inside each VC, the auxiliary variables will be optimized for B2B energy trade. After this, we reach to VC level for the optimization of auxiliary variables for B2C energy trade and the objective of VCs. In the end, the auxiliary variables for C2C are optimized. After each optimization of auxiliary variables (σ), the dual multipliers (ω) are updated. Based on the primal and dual residuals (λ^Pandλ^D), the

penalty parameters (δ) are updated. This whole process is repeated until the tolerance for dual multipliers (ω) has been reached. After calculating all the power profiles, net power injection is communicated to DSO, and the LMPs (5.34) are calculated using the DSO level problem (section 5.2.4). The new LMPs are broadcast, based on which the VCs reschedule their power profiles. This process of updating LMPs and power profiles is repeated until the convergence, i.e., the difference between the LMPs of two consecutive iterations becomes less than a tolerance threshold. Apart from the flowchart shown in Figure 5.2, a schematic view of the proposed model is also presented in Figure 5.3. This diagram depicts the overall input-output description of the model. The ultimate output is economic savings for all without violating network constraints and maintaining the data privacy of each participant.

In the proposed framework, buildings function as active participants in a decentralized energy network, where they not only consume electricity but also generate, store, and exchange it dynamically. This bidirectional energy exchange is facilitated by multiple mechanisms, ensuring an optimized, efficient, and resilient energy ecosystem. The key mechanisms enabling this B2C exchange include the following.

- Beyond intra-community energy trading, buildings can also exchange energy with buildings in other communities, fostering a larger cooperative energy network. This mechanism balances regional energy demand and supply, reducing transmission losses and increasing overall efficiency. They do the same with the help of the community,

- The inclusion of battery storage allows buildings to store excess energy when generation exceeds demand and release it when needed. These storage systems smooth out power fluctuations, reduce dependency on the grid, and enhance energy autonomy. The buildings share a single battery energy storage system (BESS) within a community. Thus, power exchange with BESS also occurs through B2C power exchange.

- Buildings are connected to the main electrical grid through the community itself, allowing them to import power during periods of low local generation and export surplus energy when they produce more than they consume. This grid interaction provides stability and flexibility, especially when renewable energy production fluctuates. Thus, buildings' energy exchange with the grid also contribute to B2C energy exchange.

By leveraging these mechanisms, the framework promotes energy efficiency, sustainability, and resilience, transforming buildings from passive consumers into dynamic energy hubs.

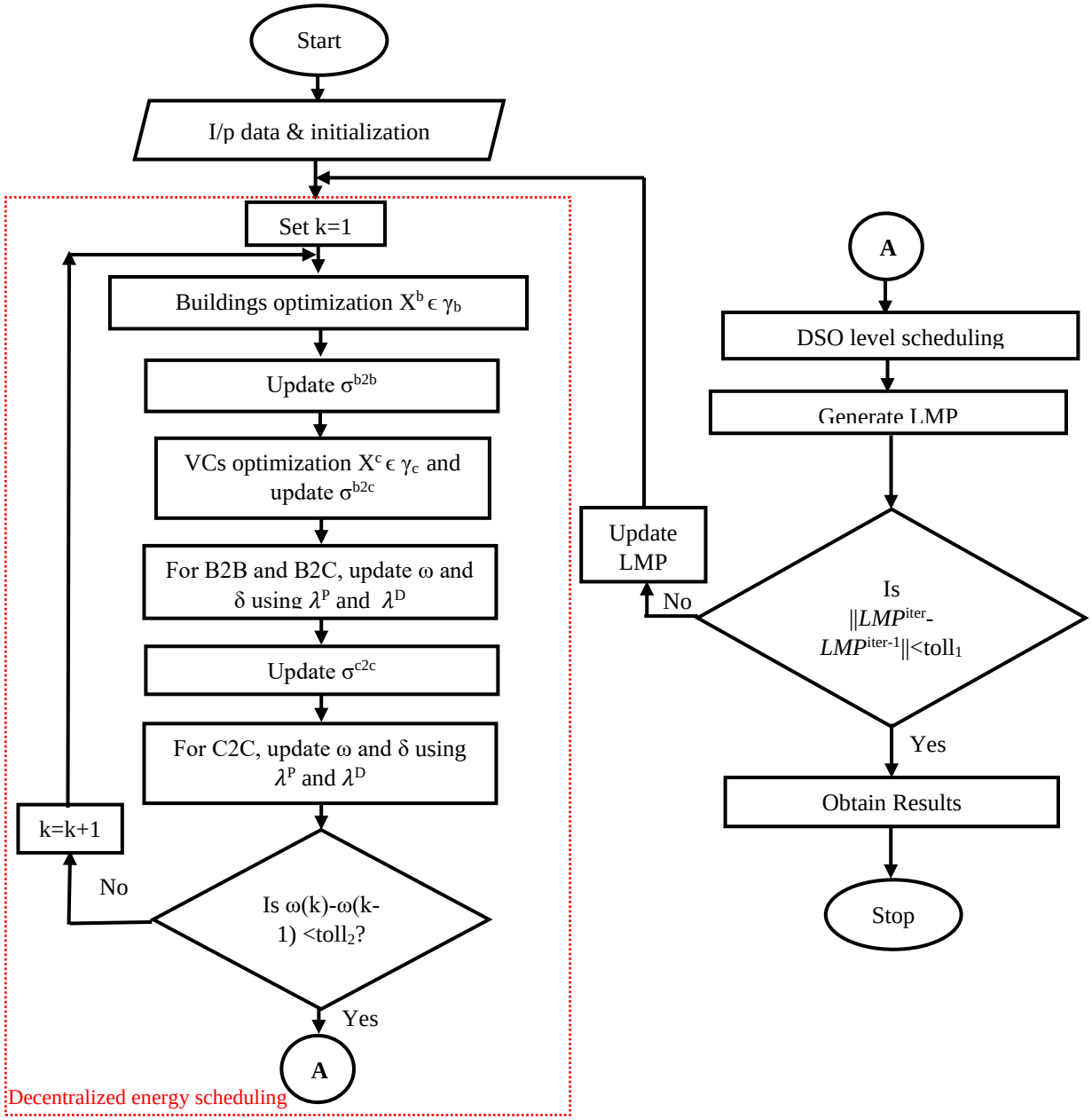

Figure 5.2: FLOWCHART FOR P2P ENERGY SHARING WITH DSO MAINTAINING THE NETWORK PARAMETERS

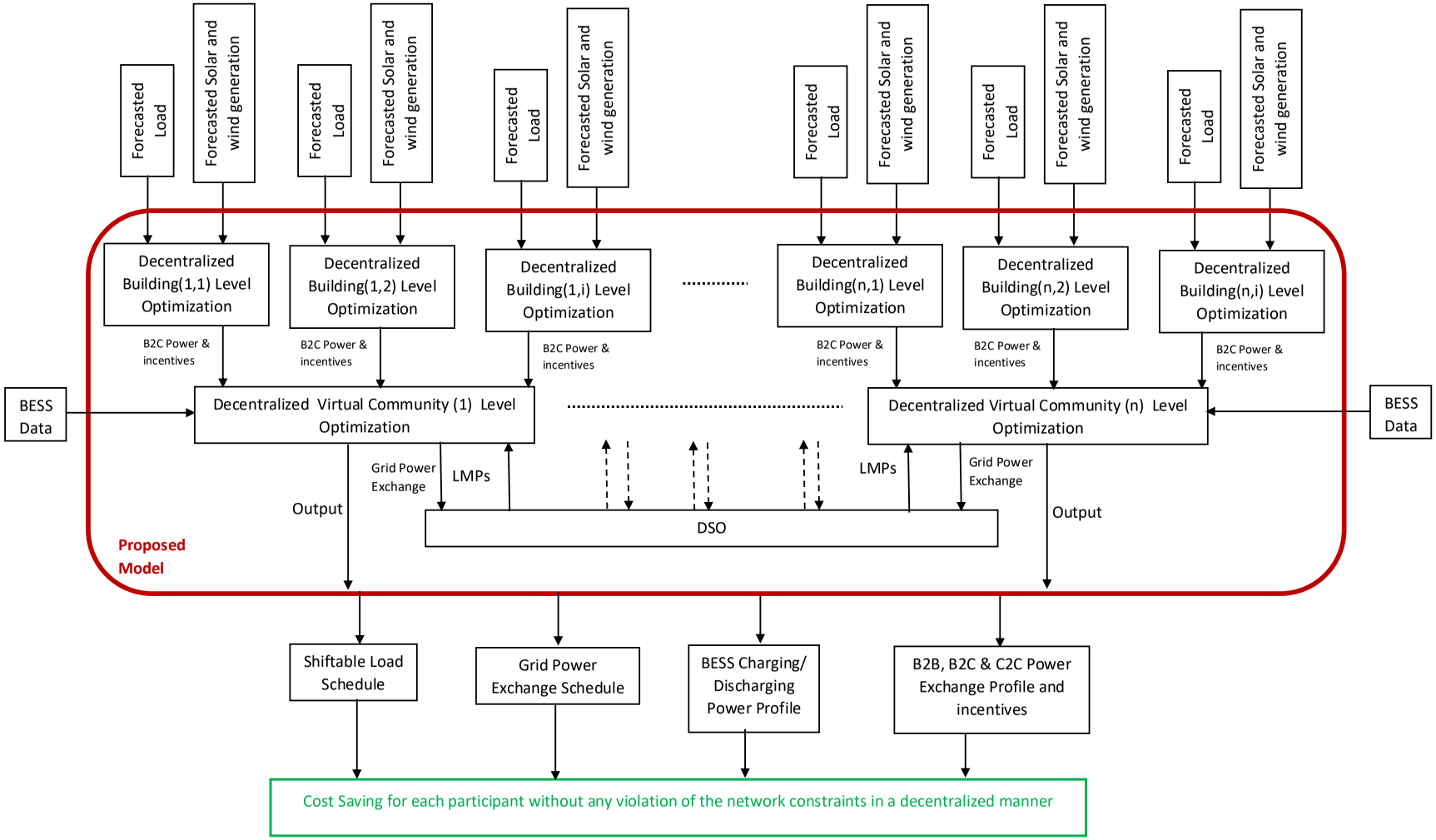

Figure 5.3: SCHEMATIC VIEW SHOWING THE VARIOUS INPUTS AND OUTPUTS OF THE PROPOSED MODEL

Table 5.3: Description of Installed capacity of Solar Power Generation (SPG), Wind Power Generation (WPG) and Battery Energy Storage System (BESS)

	VC1			VC2			VC3		
	B1	**B2**	**B3**	**B1**	**B2**	**B3**	**B1**	**B2**	**B3**
SPV (kW)	125	125	125	100	125	125	100	100	100
WPG (kW)	100	100	100	50	100	100	50	50	50
BESS (kW)	200			200			200		

5.4 Simulation Results

In this work, IEEE 33 bus system with three VCs (*VC1*, *VC2*, and *VC3*), each having three buildings (*B1*, *B2*, and *B3*) with non-identical load curves (Figure 5.4(a)) and RESs generations (Figure 5.4(b)), are considered as given in Appendix II. *VC1*, *VC2*, and *VC3* are considered on buses 21, 24, and 18, respectively. Two DGs are placed on buses 6 and 13 having cost coefficient $\Lambda_t^d = 0.32\$/kW$. In Figure 5.4(b), the wind power generation (WPG) and solar power generation (SPG) profiles are depicted for 100kW and 125kW rated capacity, respectively. The details of installed capacity of various generations are presented in Table 5.3.

The limits of SOC of the shared BESS are considered to be in the range of 20% to 90%. For all the BESSs, the discharging and charging power is limited to 50kW/h. The fraction of load supplied (ϵ^{LS}) is 1 as it is assumed that load curtailment is not present. The load can be shifted up to $\pm 10\%$. The time frame, T used for simulation is 24 hours. Other parameters are mentioned in the Table 5.4. The code is implemented on a laptop with a Core $i3$ 1.20 GHz processor with 4 GB RAM. GAMS/CONOPT4 solver is used for optimization.

Three different cases are considered to show the effectiveness of the proposed P2P framework:

Case I (Base case): All the buildings act independently and meet their load demand by shifting their load and exchanging energy only with the utility.

Case II: B2B and B2C sharing are considered in this case. A shareable BESS is present in each VC.

Case III: This case consists of an additional C2C transaction along with all the transactions considered in $Case\ II$. Also, the network utilization charge is added with every C2C energy exchange.

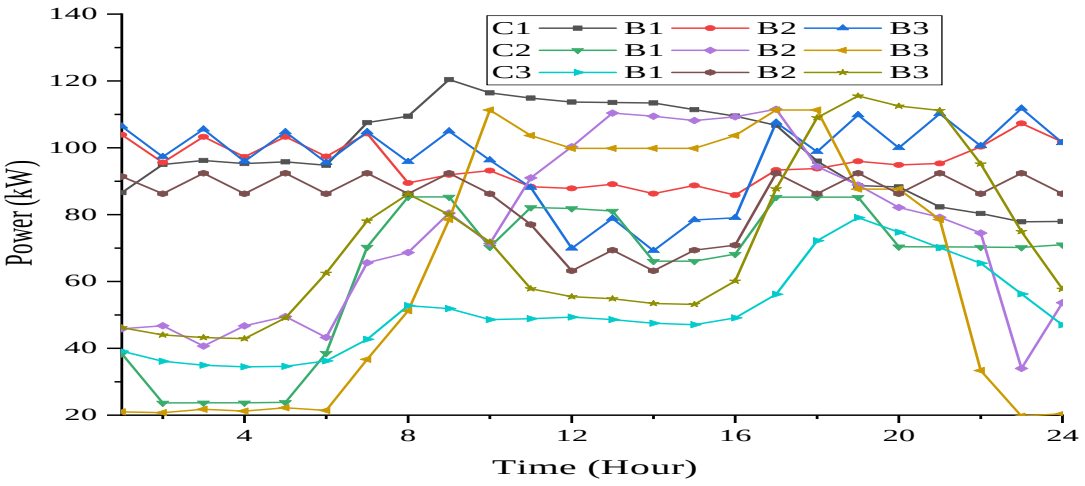

(a)

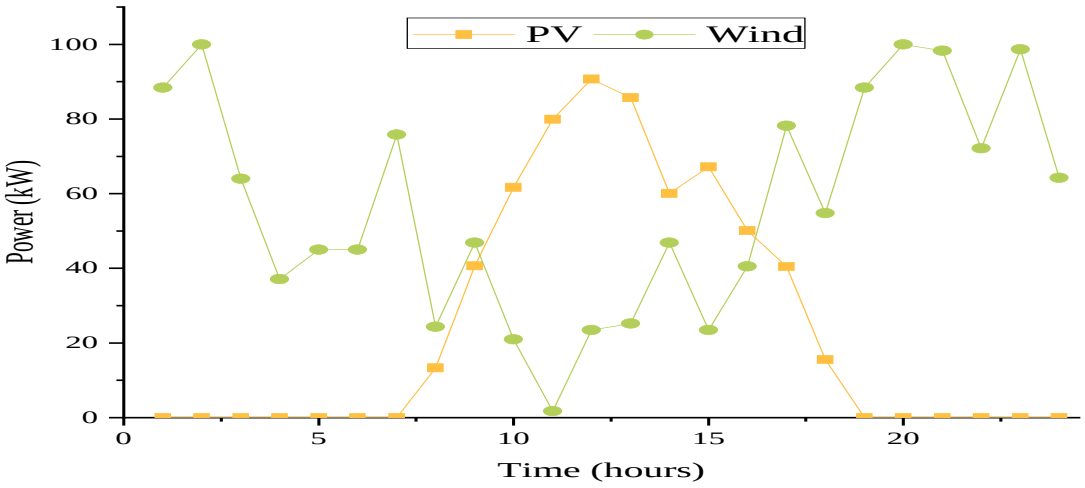

(b)

Figure 5.4: (A) LOAD CURVES OF BUILDINGS (B) RENEWABLE ENERGY SOURCES (RES) POWER GENERATION

Table 5.5 highlights a comparative analysis of costs for all three cases. $Case\ I$ exhibits the highest costs of buildings, C^b, in comparison to $Case\ II$ as well as $Case\ III$. The total operating expenses of buildings are 339.36 \$, 151.13 \$, and 528.25 \$ for *VC1*, *VC2* and *VC3*, respectively in $Case\ I$. In this case, all buildings exclusively engage in energy exchange only with the utility. Based on their respective power exchange price, which is the LMP and available RES generation, buildings shift their loads to lessen the cost.

In $Case\ II$ and $Case\ III$, buildings can exchange power among themselves and utilise BESS to manage RES effectively. Therefore, as shown in Figure 5.5, the power exchange with the utility decreases in $Case\ II$ and $Case\ III$ compared to $Case\ I$. For instance, the power

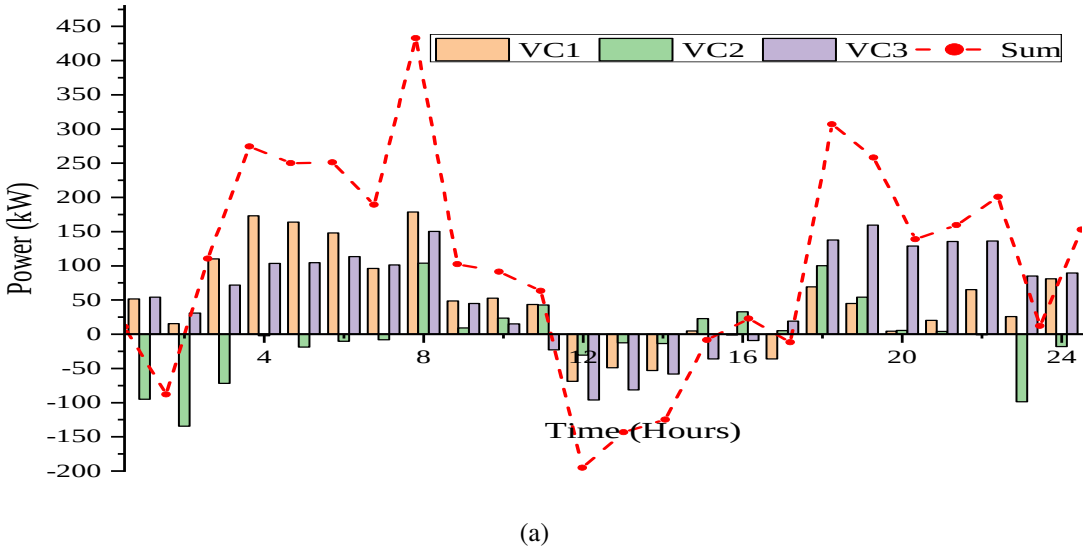

(a)

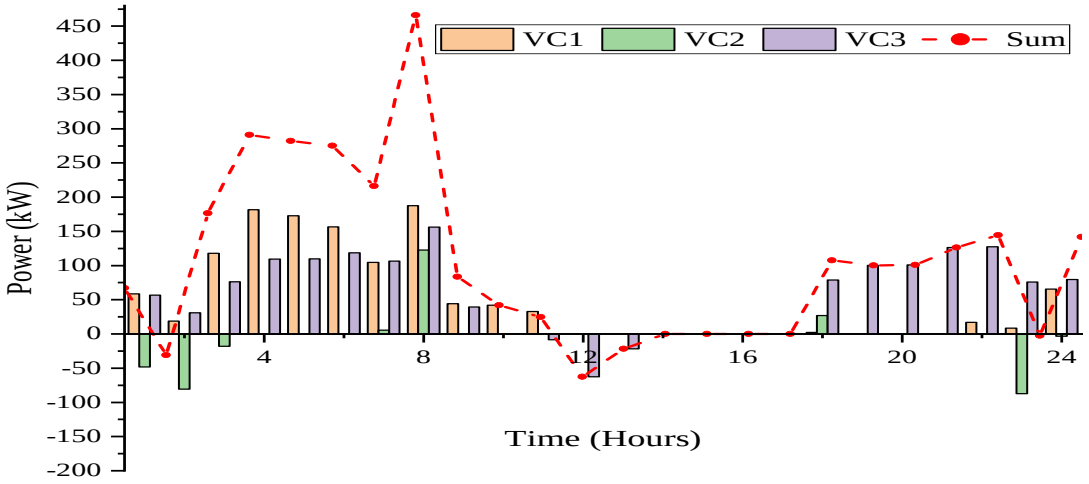

(b)

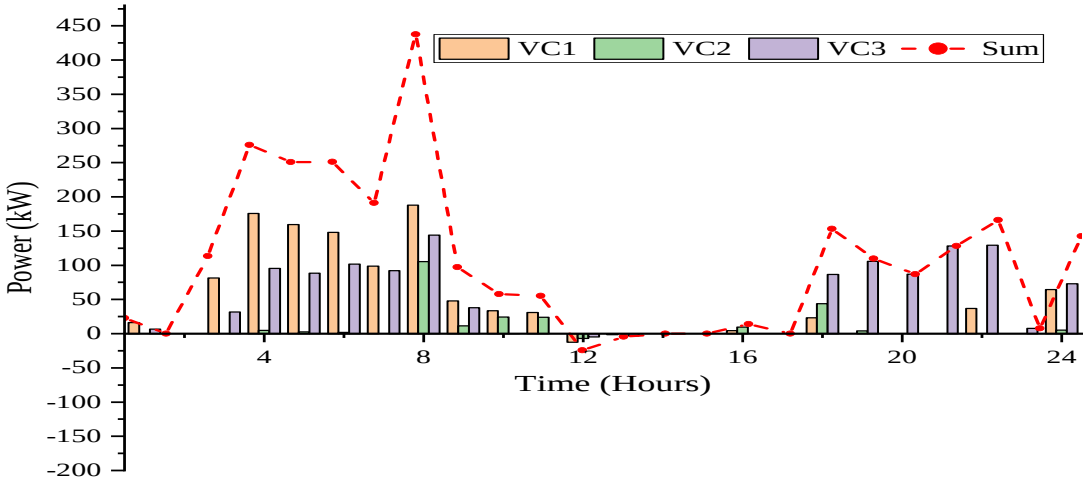

(c)

Figure 5.5: Power Exchange of VC with the Utility (a) $Case\ I$, (b) $Case\ II$, (c) $Case\ III$

Table 5.4: VALUES OF OTHER PARAMETERS USED

Parameters	Values
η^{ch}	96%
η^{dis}	94.3%
η^{loss}	0.5%
Λ^{UTI}	0.06$/kW
ϵ^{CE}	0.05$/kW
Λ^{dis}	$0.03\$/kW^2$
ϵ_R	4
σ	0.2
τ	0.01
ν	1.5

export in *VC3* decreases during 1:00 to 3:00 hours because this excess power is used to charge the BESS and to exchange in B2B transactions within the VC. The charging-discharging profile of BESS is shown in Figure 5.6(a). The BESS profile of *VC3* in $Case\ II$ depicts that the stored energy during 1:00 to 6:00 hours is used in subsequent hours of the day to satisfy the load demand. Similarly, the BESSs in other VCs are charged during the mid-day period and discharged during 17:00 to 24:00 hours. The charging/discharging of BESS depends on the RES generation. The B2B power exchange is shown in Figure 5.7. In *VC1*, *B1* imports power from other buildings of its VC during 7:00 to 17:00 hours, whereas it exports power to other buildings during the rest of the period. Similarly, *B1* in *VC2* and *B2* in *VC3* import power from other building most of the time. Therefore, the B2B costs, C^{b2b}, are positive for these buildings. The B2B power exchange depends on the individual building surplus/deficit power status, and the B2B cost depends on this B2B power exchange. However, this B2B power exchange benefits all peers because buyers can buy power at a lower cost, and sellers can sell power at a higher cost compared to the cost of power exchange with utility.

An additional option, C2C power exchange, is available in $Case\ III$. This option offers the opportunity to harness the benefits of the load diversity of buildings of other VCs. Due to this C2C power exchange, the power export to the utility further decreases compared to $Case\ II$. Figure 5.5(c) depicts that the power exported to the utility is significantly small in $Case\ III$ compared to $Case\ I$. However, at certain time instants, such as 18:00 and 22:00 hours, the

Table 5.5: Comparative analysis of costs ($)

		VC1				VC2				VC3			
		B1	**B2**	**B3**	**Sum**	**B1**	**B2**	**B3**	**Sum**	**B1**	**B2**	**B3**	**Sum**
$Case\ I$	C^b	121.11	102.57	115.68	339.36	116.58	25.28	9.26	151.13	66.95	280.23	181.07	528.25
$Case\ II$	C^{ls}	18.16	18.14	17.21	53.51	21.80	26.41	18.83	67.04	9.51	13.65	10.72	33.87
	C^{b2b}	4.79	-6.33	1.54	0.00	36.81	-15.45	-21.36	0.00	-65.48	62.49	2.99	0.00
	C^{b2c}	94.50	87.10	93.28	274.88	42.25	-1.04	-3.74	37.47	115.87	197.19	160.35	473.40
	C^b	117.46	98.91	112.02	328.39	100.86	9.92	-6.27	104.51	59.90	273.32	174.06	507.27
$C^b_{Case\ I-Case\ II}$		3.65	3.66	3.66	10.97	15.72	15.36	15.53	46.62	7.05	6.91	7.01	20.98
$Case\ III$	C^{ls}	2.38	2.32	2.24	6.93	2.20	2.44	2.12	6.76	2.31	2.33	2.32	6.96
	C^{b2b}	4.61	-6.34	1.73	0.00	39.67	-15.24	-24.43	0.00	-62.40	57.11	5.29	0.00
	C^{b2c}	93.41	85.89	91.04	270.34	41.86	5.47	-1.02	46.31	106.10	199.98	152.55	458.64
	C^b	100.40	81.87	95.01	277.27	83.73	-7.33	-23.32	53.07	46.01	259.42	160.16	465.60
$C^b_{Case\ I-Case\ III}$		20.71	20.7	20.67	62.09	32.85	32.61	32.58	98.06	20.94	20.81	20.91	62.65

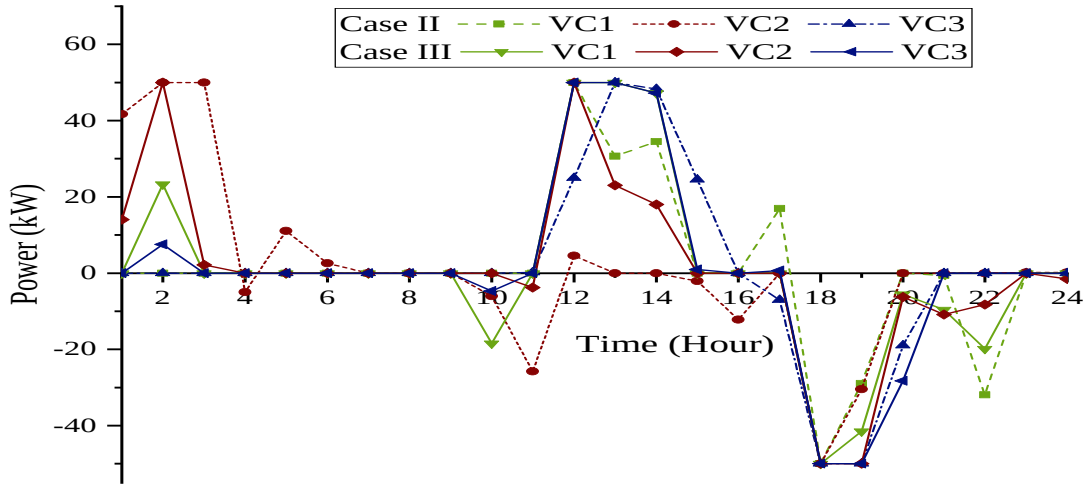

(a)

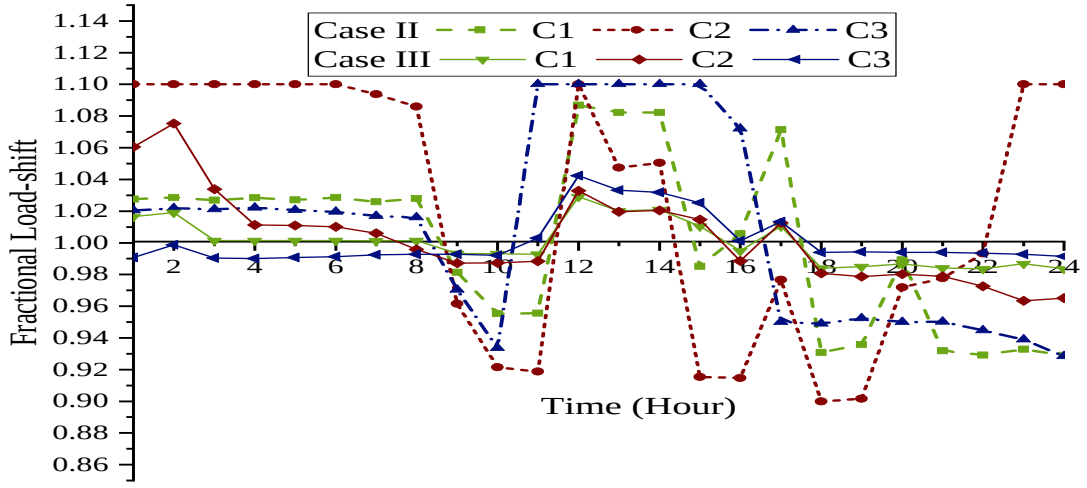

(b)

Figure 5.6: (A) CHARGE/DISCHARGE POWER OF BESSS (B) FRACTIONAL LOAD-SHIFT WITH RESPECT TO THEIR ACTUAL LOAD.

power import from the utility increases to compensate for user discomfort. The C2C energy transaction in $Case\ III$ gives a cheaper alternative to load-shifting. As shown in Figure 5.6(b), the buildings reduce load shifting in $Case\ III$ when compared with $Case\ II$. In Figure 5.6(b), the fractional load shift with respect to their actual load is shown. The cost due to load shifting, C^{ls}, is shown in Table 5.5. The C^{ls} is much lower in $Case\ III$ as compared to $Case\ II$ for buildings. The total cost of the building decreases by 15.57%, 49.22%, and 8.21% for *VC1, VC2* and *VC3* when analyzing $Case\ III$ relative to $Case\ II$. Compared to $Case\ I$, the net cost of all three communities in $Case\ III$ is decreased by a percentage of 18.3%, 64.9%, and 11.9%, respectively.

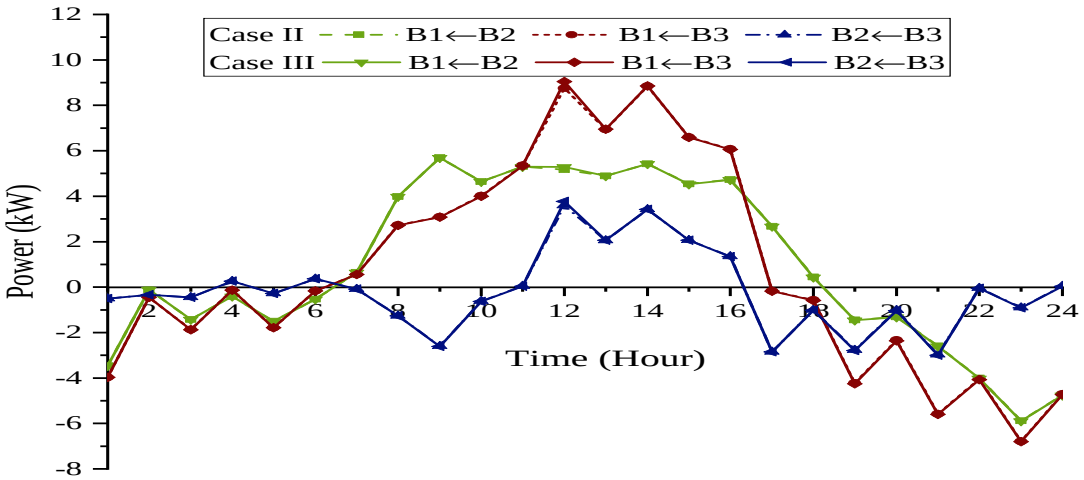

(a)

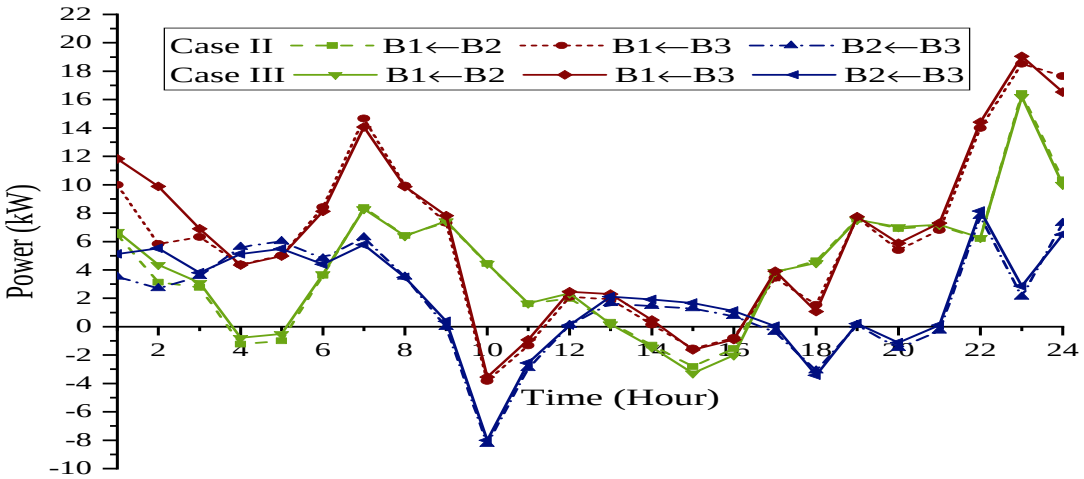

(b)

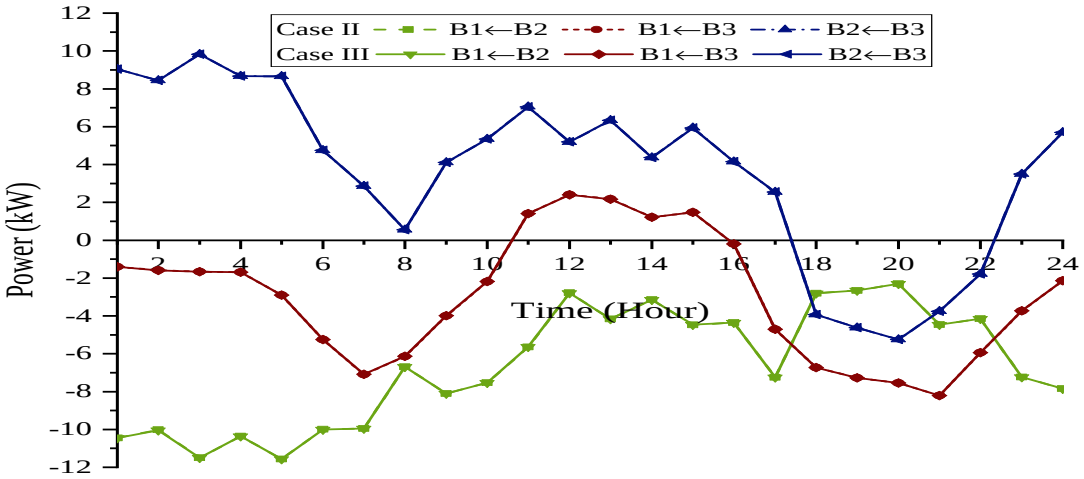

(c)

Figure 5.7: POWER EXCHANGE IN B2B ENERGY TRADING FOR *CASE II* AND *CASE III* (A) *VC1*, (B) *VC2*, (C) *VC3*

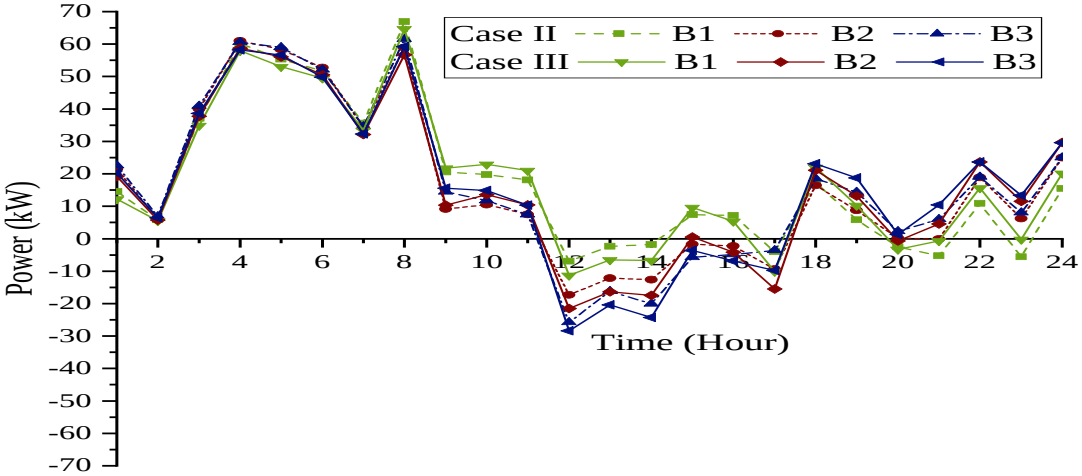

(a)

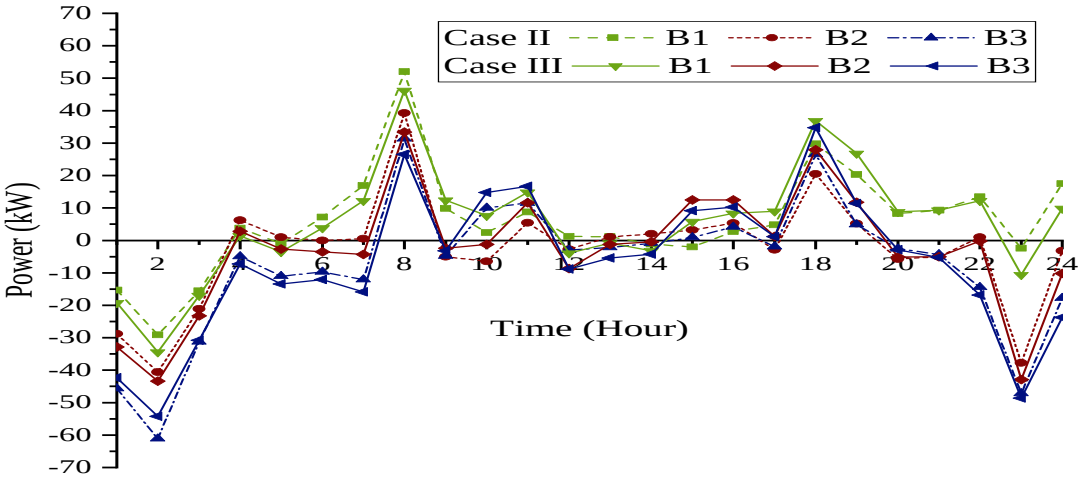

(b)

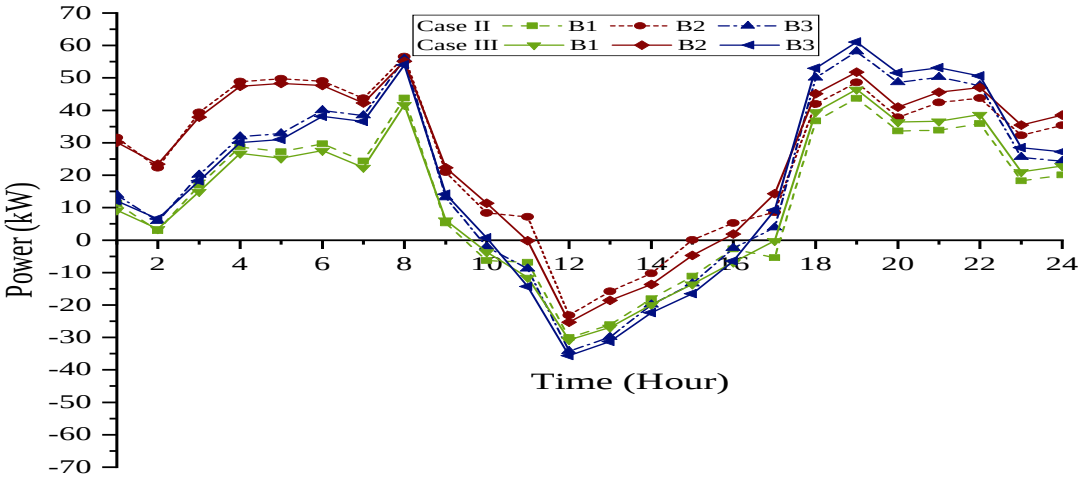

(c)

Figure 5.8: Power Exchange in B2C energy trading (a) *VC1*, (b) *VC2*, (c) *VC3*

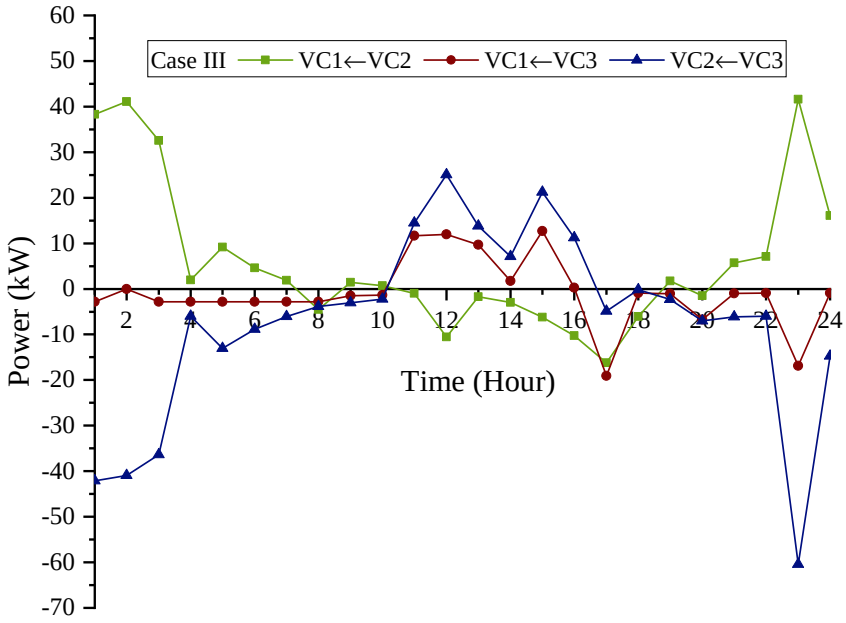

(a)

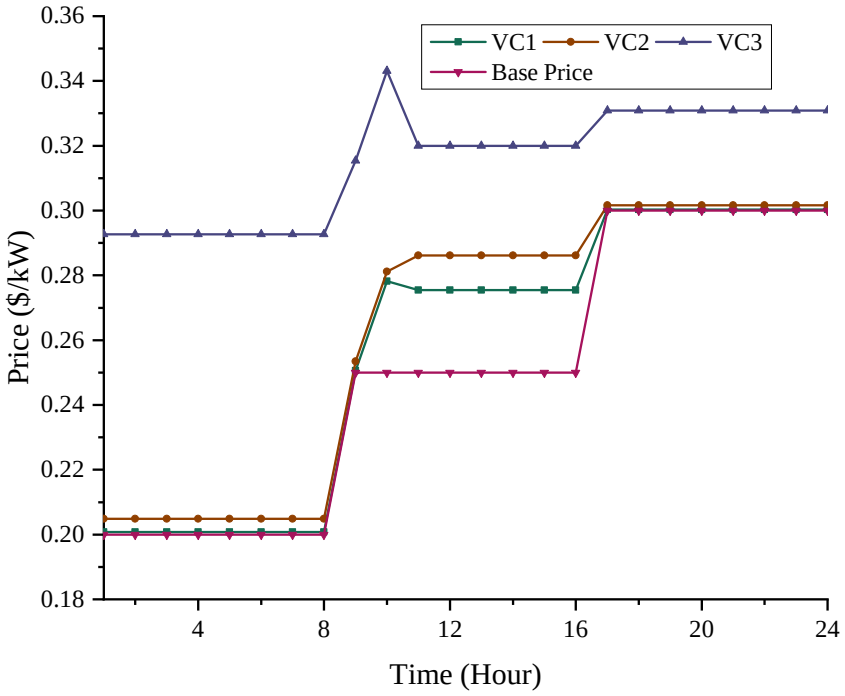

(b)

Figure 5.9: (A) C2C NET POWER EXCHANGE, (B) LMPS OF THREE VCS AND THE BASE PRICE

As depicted in Figure 5.6(b), at most of the time instants, the increment in load demand occurs from 1:00 to 16:00 hours for all VCs, and the decrement in load demand occurs after 16:00 hours in $Case\ II$ due to surplus RES and low tariff period. In this case, the only option for VCs is to consume excess RES generation locally or export it to the utility. But, in $Case\ III$, they prefer inter-VC power exchange rather than load-shifting. Therefore, as shown in Figure 5.8, in $Case\ III$, the power import decreases during 1:00-10:00 hours, whereas it decreases during 17:00-24:00 hours. As far as power export is concerned in $Case\ III$, it invariably increases, as seen in Figure 5.8. Figure 5.6(a) shows that in $Case\ III$, due to the cumulatively surplus energy during 11:00 to 15:00 hours, most BESS charging occurs from 11:00 to 15:00 hours. Figure 5.5(b) shows that *VC2* has surplus energy during 1:00-3:00 hours even after BESS charging. This surplus energy and energy stored due to the shifting of BESS charging is utilised to export to the other VCs. Figure 5.9(a) shows the inter-VC energy exchange. The *VC2* only imports power from other VCs during 12:00-16:00 hours, which is used to charge the BESS. The total incentives for C2C energy trading in $case\ III$ for *VC1, VC2*, and *VC3* are 5.76$, -46.67$, and 40.91$ respectively. As shown in Figure 5.9(a), except for 8:00 to 18:00 hours, *VC2* always exports to the other VCs. Therefore, the total C2C incentive for *VC2* is negative compared to other VCs. It means that the *VC2* gets incentives from other VCs. The proposed framework considers the power exchange profile of VCs to calculate the LMPs. The LMPs for three VCs are depicted in Figure 5.9(b) for $Case\ III$. The LMP of *VC3* is highest because it is connected at 18^{th} bus. The voltage level at 18^{th} bus is the lowest and closer to voltage limit violation.

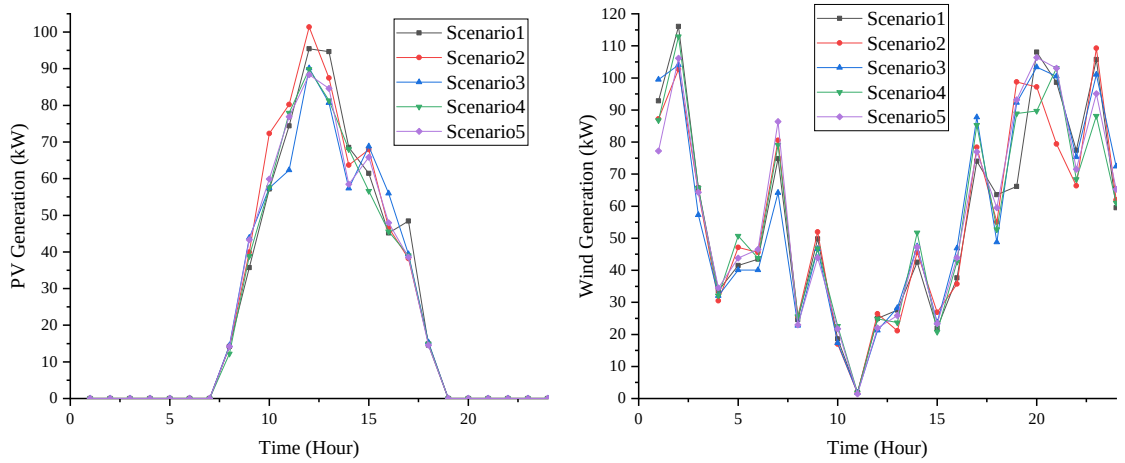

(a) (b)

Figure 5.10: FIVE RANDOM SCENARIOS FOR (A) PV AND (B) WIND GENERATION RESPECTIVELY

Table 5.6: NET SAVING ($) IN FIVE DIFFERENT SCENARIOS

Virtual Community		**VC1**			**VC2**			**VC3**		
Building		**B1**	**B2**	**B3**	**B1**	**B2**	**B3**	**B1**	**B2**	**B3**
Scenario 1	$C^b_{Case\ I}$	115.34	95.83	108.24	112.33	18.28	9.28	60.55	276.17	174.80
	$C^b_{Case\ III}$	97.78	78.27	90.69	87.97	-6.37	-15.08	39.69	255.37	153.97
	Net Saving	**17.56**	**17.56**	**17.55**	**24.36**	**24.64**	**24.36**	**20.87**	**20.80**	**20.84**
Scenario 2	$C^b_{Case\ I}$	107.06	88.68	102.30	108.08	12.67	-0.49	59.76	272.24	173.41
	$C^b_{Case\ III}$	91.89	73.51	87.17	80.11	-15.23	-28.38	41.74	254.25	155.40
	Net Saving	**15.17**	**15.17**	**15.12**	**27.96**	**27.90**	**27.89**	**18.03**	**17.99**	**18.02**
Scenario 3	$C^b_{Case\ I}$	114.08	94.97	108.58	110.71	15.89	5.28	62.28	274.82	175.54
	$C^b_{Case\ III}$	96.65	77.54	91.15	85.22	-9.60	-20.17	42.86	255.50	156.17
	Net Saving	**17.43**	**17.43**	**17.43**	**25.49**	**25.49**	**25.45**	**19.42**	**19.33**	**19.38**
Scenario 4	$C^b_{Case\ I}$	114.70	99.81	111.98	116.79	18.50	7.69	64.11	280.25	179.27
	$C^b_{Case\ III}$	98.48	83.58	95.76	93.72	-4.60	-15.39	43.31	259.55	158.53
	Net Saving	**16.23**	**16.23**	**16.22**	**23.07**	**23.10**	**23.07**	**20.80**	**20.70**	**20.75**
Scenario 5	$C^b_{Case\ I}$	108.13	89.06	102.00	108.18	11.53	0.88	57.34	272.81	172.90
	$C^b_{Case\ III}$	88.62	69.55	82.49	80.39	-16.26	-26.90	36.54	252.03	152.11
	Net Saving	**19.51**	**19.51**	**19.51**	**27.79**	**27.79**	**27.78**	**20.79**	**20.78**	**20.79**

Table 5.7: NET SAVING ($) IN DIFFERENT SEASONS OF THE YEAR

Virtual Community		**VC1**			**VC2**			**VC3**		
Buildings		**B1**	**B2**	**B3**	**B1**	**B2**	**B3**	**B1**	**B2**	**B3**
Season 1	$C^b_{Case\ I}$	284.64	293.21	307.55	200.01	182.37	126.09	180.72	383.78	293.91
	$C^b_{Case\ III}$	283.35	291.92	306.25	198.47	180.82	124.55	176.60	379.66	289.79
	Net Saving	1.29	1.29	1.29	1.54	1.54	1.54	4.12	4.12	4.12
Season 2	$C^b_{Case\ I}$	86.58	87.16	100.23	97.61	17.30	-0.49	52.55	245.29	150.44
	$C^b_{Case\ III}$	72.25	72.83	85.90	77.02	-3.13	-20.65	35.61	228.03	133.36
	Net Saving	14.33	14.33	14.33	20.59	20.43	20.16	16.94	17.27	17.08
Season 3	$C^b_{Case\ I}$	92.14	106.65	122.18	101.62	34.61	24.13	61.67	244.53	156.28
	$C^b_{Case\ III}$	79.72	94.23	109.76	81.12	14.12	3.65	47.01	228.18	140.85
	Net Saving	12.42	12.42	12.42	20.51	20.49	20.48	14.66	16.35	15.43
Season 4	$C^b_{Case\ I}$	103.21	117.20	131.62	113.25	39.76	22.61	68.41	255.87	167.69
	$C^b_{Case\ III}$	94.00	107.98	122.40	96.99	23.78	6.87	55.62	241.24	153.79
	Net Saving	9.22	9.22	9.22	16.26	15.98	15.74	12.79	14.63	13.90

For robustness analysis of the proposed model, five different forecasted scenarios have been used for solar generation (SPG) and wind generation (WPG). Figure 5.10 shows the scenarios for 125 kW rated capacity WPG and 100 kW rated SPG. Table 5.6 shows that there is little deviation in the net savings of all buildings across different scenarios, and the proposed framework ensures economic benefits to all buildings in all scenarios. The proposed framework has also been used to study the seasonal variation. From the reference [78], seasonal data of solar and wind generation have been used in modified form for this model. The model is optimised, and the results are recorded in Table 5.7 for a particular day of each season. Table 5.7 also indicates the robustness of the model by resulting in sufficient net savings in all the seasons for all the buildings.

5.5 Summary

For VCs having several buildings and a shareable BESS, a cost-saving P2P energy management scheme is proposed in this chapter. Aggregating buildings in VCs reduces the number of transactions, thereby enhancing the system's scalability. The numerical results establish the efficacy of the proposed energy trading framework in realizing the benefits of P2P sharing. Adopting the proposed LMP-based P2P sharing framework yields a significant reduction in the net energy cost of all buildings without breaching network constraints. The proposed P2P sharing increases the value of RESs usage and reduces the power exchange with utility as it provides an opportunity to take advantage of the load diversity of all buildings. Also, uncertainty associated with RESs generation is handled effectively. In $Case\ III$ compared to $Case\ I$, the net cost of all three communities is decreased by a percentage of 18.3%, 64.9%, and 11.9%, for $VC1$, $VC2$, and $VC3$, respectively.

In this chapter, for maintaining the network constraints, it is assumed the DSO takes the help of DGs, which are directly under the control of DGs. DSO in real-life scenarios, the DGs are profit-based independent entities. This fact has been further explored in later chapters.